

# Fabrication of TiO<sub>2</sub> nanotubes by using electrodeposited ZnO nanorod template and their application to hybrid solar cells

Seok-In Na, Seok-Soon Kim, Woong-Ki Hong, Jeong-Woo Park, Jang Jo,  
Yoon-Chae Nah, Takhee Lee, Dong-Yu Kim\*

*Heeger Center for Advanced Materials, Department of Materials Science and Engineering, Gwangju Institute of Science and Technology (GIST), Gwangju 500-712, South Korea*

Received 16 August 2007; received in revised form 10 October 2007; accepted 14 October 2007

Available online 25 October 2007

## Abstract

Vertically aligned TiO<sub>2</sub> nanotubes have been fabricated on the indium-doped tin oxide (ITO) by a simple and versatile technique using the electrochemically deposited ZnO nanorods, oriented along the *c*-axis, as a template in the spin-on based sol–gel reaction of a Ti precursor. The diameter, length, and shape of TiO<sub>2</sub> nanotubes were controlled by changing the initial ZnO nanorod template and the spin conditions during sol–gel process of a Ti precursor. Scanning electron microscopy (SEM), energy-dispersive X-ray (EDX) analysis, and X-ray diffraction (XRD) were used to confirm the successful formation of TiO<sub>2</sub> nanotubes and characterize their structure and morphology. Furthermore, as an application of the TiO<sub>2</sub> nanotubes, hybrid solar cells based on TiO<sub>2</sub> and poly[2-methoxy,5-(2'-ethyl-hexyloxy)1,4-phenylenevinylene] (MEH-PPV) were successfully fabricated.

© 2007 Elsevier Ltd. All rights reserved.

**Keywords:** Electrodeposition; Zinc oxide nanorod; Sol–gel process; Titanium dioxide nanotubes; Hybrid solar cells

## 1. Introduction

Since the introduction of carbon nanotubes by Iijima in 1991 [1], various nanotubes and tubular nanostructures continue to attract attention due to a high surface-to-volume ratio, structural control capabilities, and a geometry that functions as a current-carrying component in various devices. They also have remarkable optical, electrical, magnetic, and chemical properties that are distinctive from conventional bulk materials and zero-dimensional nanoparticles [2–4]. For more than a decade, investigations on the synthesis and characterization of many kinds of nanotubes, such as boron nitride and carbide, metal dichalcogenide, SiO<sub>2</sub>, SnO<sub>2</sub>, GaN, ZnO, TiO<sub>2</sub>, ZrO<sub>2</sub>, and vanadium oxides, have been reported [2–8]. In particular, among the various inorganic nanotubes, the TiO<sub>2</sub>-based nanotube has been intensively studied for potential nanoscale electronics, optoelectronics and biochemical-sensing applications due to its high

refractive index, chemical stability, and superior photocatalytic activity [9–12].

Up to now, much effort has been devoted to forming TiO<sub>2</sub> nanotubes by using hydrothermal synthesis [13,14], deposition on template [15–19], seeded-growth [20], and anodization of titanium [9,21]. Specially, in the case of the anodic TiO<sub>2</sub> nanotubes, a precise control of the TiO<sub>2</sub> tube dimensions and the feasibility of TiO<sub>2</sub> nanotubes to be formed on Si substrate have been reported for their practical applications [22,23]. Although each of the above-mentioned methods has advantages, none of them provide all the desired aspects: precise control of the nanotube configuration, dense arrays of vertical or parallel-aligned TiO<sub>2</sub> nanotubes, low cost, a high throughput process, and feasibility of their use in a large area as well as on widely used substrates such as glass, silicon, and transparent conducting oxide (TCO). Therefore, the pursuit of novel fabrication methods for nanotubes continues to be driven by an ever-increasing world of practical device applications.

Among various methods for fabricating TiO<sub>2</sub> nanotubes, few efforts have been made on the study of use of ZnO nanorods as a template. Very recently, Qiu et al. [18,19] successfully

\* Corresponding author. Tel.: +82 62 970 2319; fax: +82 62 970 2304.  
E-mail address: [kimdy@gist.ac.kr](mailto:kimdy@gist.ac.kr) (D.-Y. Kim).

fabricated aligned TiO<sub>2</sub> nanotube arrays by using an aqueous solution synthesized ZnO rod as a template. However, the formation of ZnO nanorod array by an aqueous solution synthesis requires long time (~5 h) and the fabrication of pure TiO<sub>2</sub> tubes vertically aligned on a substrate is difficult due to the existence of the ZnO seed layer, which also can be etched by acidic solution when removing ZnO rod templates, leading to the collapse of TiO<sub>2</sub> tubes.

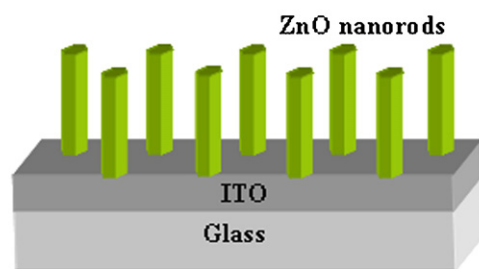
For this study, a simple and controllable fabrication method is described for vertically aligned TiO<sub>2</sub> nanotubes having well-controlled dimensions directly on indium-doped tin oxide (ITO) substrates, which are transparent electrodes widely used in optoelectronics such as solar cells and light emitting diodes. We used electrodeposited ZnO nanorods as a template for the fabrication of TiO<sub>2</sub> nanotubes, because growing of one-dimensional ZnO nanorods by electrodeposition is a simple, fast, and low-temperature method with easy control of density, diameter, and height over large areas [24,25] in contrast with vacuum and high temperature processes. As is well known, the diameters and heights of electrodeposited ZnO nanorods can be determined by experimental conditions such as the concentration of the Zn precursor, the electrodeposition time, the temperature, and the applied voltage [26,27]. In addition, we take advantage of the spin-on based sol–gel reaction of a Ti precursor, leading to the formation of a well-aligned, discrete, and freestanding TiO<sub>2</sub> nanotube array by controlling the rate of hydrolysis of the Ti isopropoxide, based on the conditions used in the previous reports by our group [28,29]. In contrast with any vacuum techniques, the sol–gel process provides low cost and high throughput, which are the most significant factors for practical use.

Organic-based solar cells [30,31] are attracting enormous attention as a low-cost, lightweight, and scalable source of renewable energy. For the realization of commercialized organic solar cells, most of the work on organic-based solar cells to date has focused on fundamental problems such as relatively low efficiency and poor stability that must be overcome [32–38]. For example, in hybrid solar cells, various approaches including the application of an ordered nanostructure [32], the substitution of magnesium into a ZnO acceptor [34], and an effort to understand polymer degradation [37] have been studied to improve cell efficiency and stability. Herein, we investigated the application of TiO<sub>2</sub> nanotubes to hybrid solar cells based on TiO<sub>2</sub> and poly[2-methoxy,5-(2'-ethyl-hexyloxy)1,4-phenylenevinylene] (MEH-PPV). An improved performance of hybrid solar cells can be expected by using the TiO<sub>2</sub> nanotube array on the ITO substrate, resulting from an extended interfacial area for charge separation and a straight pathway for electron transport to the ITO electrode.

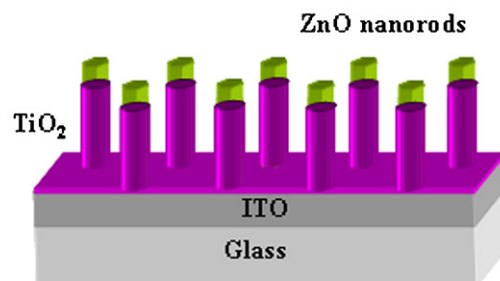
## 2. Experimental

All the chemicals were purchased from Aldrich. The process we used to create TiO<sub>2</sub> nanotubes on ITO substrates involved three main steps (Fig. 1): first, ITO (Samsung Corning Co., Ltd.) coated glass substrates were cleaned in ultrasonic bath with acetone and isopropyl alcohol successively for 20 min followed by drying in a nitrogen stream. The ZnO nanorods were then

### Growth of ZnO nanorods on ITO



### TiO<sub>2</sub> formation on ZnO nanorods



### Removal of ZnO nanorods by wet etching

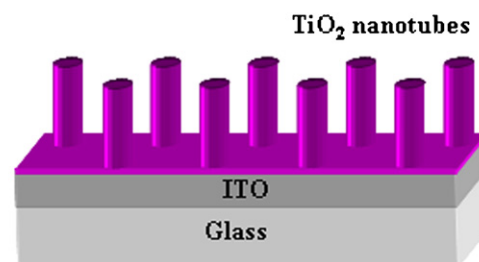


Fig. 1. Schematic process flow for the fabrication of the TiO<sub>2</sub> nanotubes.

electrodeposited on ITO substrates at  $-0.9$  V versus Ag/AgCl electrode from an aqueous solution composed of  $5 \times 10^{-3}$  M ZnCl<sub>2</sub> and 0.1 M KCl supporting electrolyte in ultra-pure water ( $\sim 18$  M $\Omega$ cm), saturated with bubbling oxygen at 80 °C [39] with an Autolab PGSTAT30 Potentiostat/Galvanostat. Here, an ITO substrate, a Pt wire, and an Ag/AgCl were used as the working, the counter, and the reference electrodes, respectively. The overall deposition reaction in the presence of zinc ions and dissolved oxygen is  $\text{Zn}^{2+} + 0.5\text{O}_2 + 2\text{e}^- \rightarrow \text{ZnO}$ .

Second, the process for the formation of TiO<sub>2</sub>-covered ZnO nanorod arrays on ITO substrates was performed via spin-on based sol–gel reaction at room temperature with the Ti-precursor composed of 2 ml Ti isopropoxide in 150 ml 2-propanol solution containing 0.75 ml HCl. To fabricate TiO<sub>2</sub>-covered ZnO nanostructures, the Ti-precursor solution was dropped on the ITO substrates with freestanding ZnO nanorods and then spun at room temperature, followed by heat treatment at 450 °C for

30 min in a furnace to form the TiO<sub>2</sub> crystalline structures. Here, the ratio of each component was optimized to control the rate of hydrolysis of Ti isopropoxide and prevent the unnecessary wet-etch of ZnO nanorods during the spin coating process, resulting in well-defined and vertically aligned TiO<sub>2</sub>-covered ZnO nanorod arrays [28,40–41].

Third, after heat treatment, the ITO substrates with TiO<sub>2</sub>-covered ZnO nanorods were immersed into an aqueous solution of 0.75 M HCl to remove the ZnO nanorod template. After the immersion in HCl solution for 5 min at room temperature, all ZnO was etched out and only the TiO<sub>2</sub> nanotubes remained, due to selective wet etching in the acidic conditions. After all processes, the formation and structure of TiO<sub>2</sub> nanotubes were confirmed by SEM (Hitachi S-4700), EDX analysis, and XRD.

For an application of fabricated TiO<sub>2</sub> nanotubes, hybrid solar cells were fabricated according to the following procedure. Two types of TiO<sub>2</sub> covered ITO substrates were prepared by a spin-on based sol–gel reaction without and with ZnO nanorod templates. For hybrid solar cells, MEH-PPV (1 wt%) in chlorobenzene, which generates excitons under illumination, was spin-cast on the flat TiO<sub>2</sub> film with thickness of ~100 nm and TiO<sub>2</sub> nanotube arrays at 500 rpm in a N<sub>2</sub> glove box. Poly(3,4-ethylenedioxythiophene):poly(styrenesulfonate) (PEDOT:PSS, Baytron P CH 8000) was then spin-cast with a thickness of ~50 nm from an aqueous solution on the substrates, after passing through a 0.45 μm filter and mixing for 1 h. After drying for 10 min at 120 °C in air, an Au top electrode was evaporated thermally in a vacuum in the order of 10<sup>-6</sup> Torr. The optical properties of MEH-PPV and TiO<sub>2</sub> nanotubes coated with MEH-PPV were studied via UV–vis absorption spectra and PL spectra measurements. Cell performance was measured under 1 sun using a xenon light source and an air mass (AM) 1.5 global filter. Photocurrent–voltage measurements were performed by using a Keithley 4200 instrument. A calibrated silicon reference solar cell certificated by the National Renewable Energy Laboratory (NREL) was used to confirm the measurement conditions.

### 3. Results and discussion

The preparation of initial ZnO nanorods as templates and successful formation of TiO<sub>2</sub> nanotubes on ITO were observed by scanning electron microscopy (SEM) images and the element signatures of Zn, Ti, and O in the energy-dispersive X-ray (EDX) spectra of the ZnO nanorods and TiO<sub>2</sub> nanotubes. Fig. 2(a) shows SEM images of the starting ZnO nanorod array templates. These nanorods have uniform lengths of ~600 nm and diameters of 170 ± 20 nm, which can be determined by concentration of the Zn precursor, applied voltage, and time during electrodeposition. Here, the applied voltage, time, and temperature were controlled to -0.9 V, 30 min, and 80 °C, respectively.

After the formation of TiO<sub>2</sub>, the heat treatment, and template removal by the wet etching, the overall morphology of the initial ZnO nanorod arrays was maintained and the heights and diameters of the resulting TiO<sub>2</sub> nanotubes were similar to those of the ZnO nanorods as shown in Fig. 2(a), (c), and (e). Indeed, the cross-sectional images in the insets of Fig. 2(a) and (e) indicate that the vertically aligned TiO<sub>2</sub> nanotubes on ITO were rela-

tively well defined along ZnO nanorod templates. At this point, for the formation of denser and better-defined TiO<sub>2</sub> nanotubes on ITO substrates, the concentration of the Ti-precursor and the spin conditions, as well as initial conditions of the ZnO nanorod templates, should be carefully considered and optimized.

Interestingly, either top-closed or top-opened TiO<sub>2</sub> nanotubes were observed according to the spin rate (slow (1000 rpm) or fast (3000 rpm)) during the spin-on based sol–gel process as shown in Fig. 2(c) and (e) and the insets of Fig. 2(c) and (f), respectively. It may be attributed to the fact that the amount of remaining Ti-precursor on the top of the ZnO nanorod template was inversely dependent on the spin rate because the Ti-precursor solution would be forced to move in the lateral direction during the spin coating process [42], which resulted in the top-opened TiO<sub>2</sub> nanotubes.

Fig. 2(b), (d), and (f) shows the EDX spectra before and after the formation of TiO<sub>2</sub> nanotubes. The EDX spectra revealed the successful formation of TiO<sub>2</sub> nanotubes and the complete elimination of the ZnO nanorods as a template, confirmed by the absence of a peak at ~1 keV corresponding to the Zn in the EDX spectra obtained from the sample area shown in the insets of Fig. 2(d) and (f). The formation of TiO<sub>2</sub> can also be confirmed by the measurement of X-ray diffraction (XRD) patterns. Fig. 3 shows the XRD patterns obtained from the TiO<sub>2</sub> nanotube arrays on the ITO substrate. After calcination at 450 °C in air and removal of ZnO rod templates, all peaks apparently corresponded to anatase TiO<sub>2</sub> (JCPDS Card no. 21-1272) and ITO (JCPDS Card no. 32-0458), indicating that the ZnO rod templates were completely removed by the wet etching and the TiO<sub>2</sub> nanotubes were successfully fabricated.

Taken together, the above SEM, EDX, and XRD measurements show that we have successfully prepared vertically well-aligned TiO<sub>2</sub> nanotubes on ITO substrates by using all solution processes, including the formation of the electrodeposited ZnO nanorod from an aqueous solution, the formation of TiO<sub>2</sub> nanotubes by spin-on based sol–gel reaction of a Ti-precursor, and the removal of a ZnO template by immersion in an acidic solution environment, instead of using any vacuum processes, such as atomic layer deposition or chemical vapor deposition, etc.

Furthermore, to demonstrate practical application of the TiO<sub>2</sub> nanotubes, hybrid solar cells based on TiO<sub>2</sub> nanotubes and MEH-PPV were prepared. Typically, the TiO<sub>2</sub>, one of the most widely exploited inorganic materials due to its low cost, chemical stability, electron accepting ability, and proper band gap, is prepared on a TCO substrate by a casting or sol–gel method followed by infiltration with a conjugate polymer [43–48]. In early studies, the incomplete polymer infiltration into nanoporous TiO<sub>2</sub> and poor charge transport, resulting from the randomly networked TiO<sub>2</sub> nanoporous film, could be main factors causing the poor performance of hybrid solar cells. To overcome these problems, various approaches including the application of an ordered nanostructure have been intensively investigated to achieve a large interfacial area and straight carrier paths to the electrodes as well as an easy polymer infiltration [49–51]. Therefore, with its vertical array, standing on ITO substrates, the TiO<sub>2</sub> nanotube is a good candidate for use as an electron

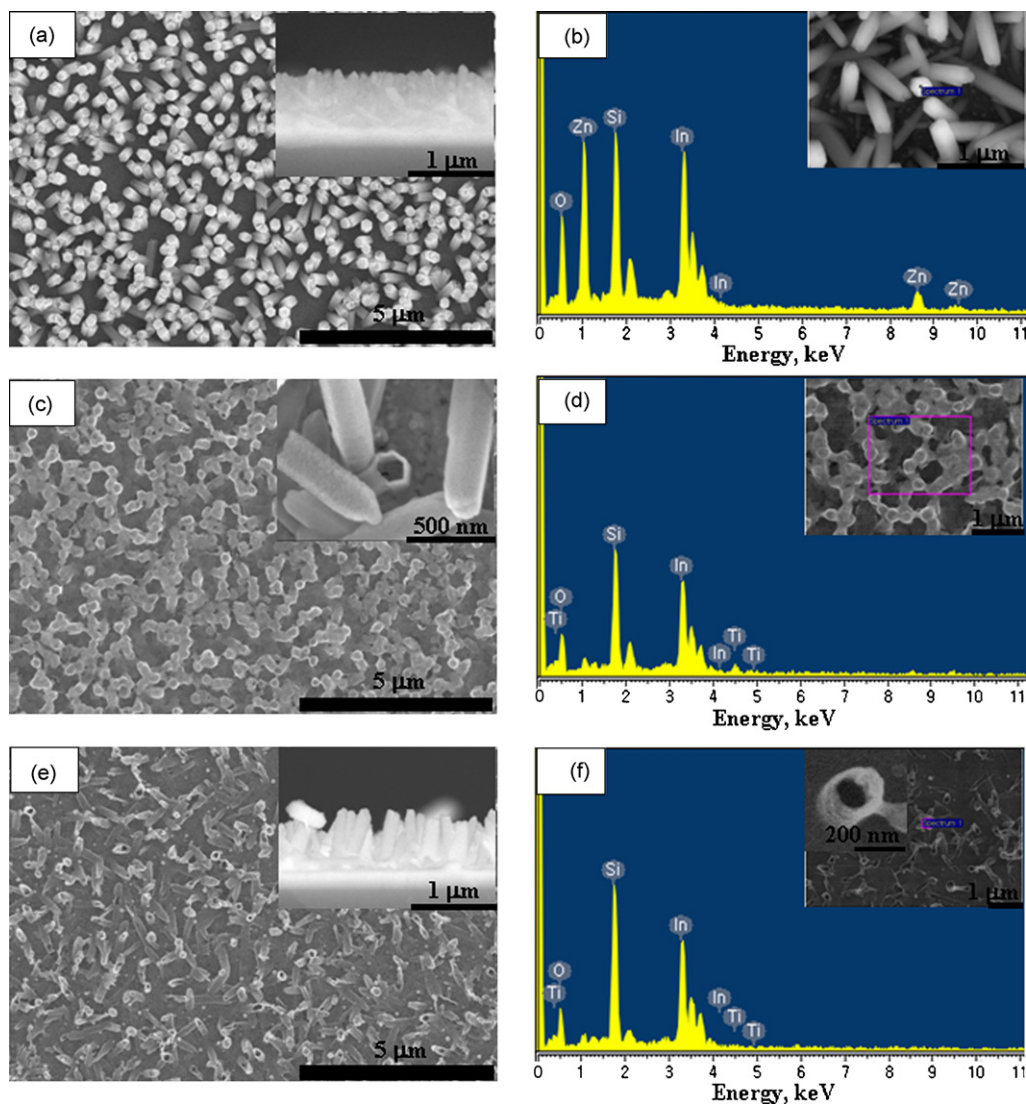


Fig. 2. FESEM images and EDX spectra: (a) and (b) ZnO nanorods on ITO substrates before the formation of TiO<sub>2</sub> nanotubes; (c)–(f) corresponding images and spectra after the formation of TiO<sub>2</sub> nanotubes with different spin coating rate via the spin-on based sol–gel reaction of Ti-precursor solution followed by heat treatment and removal of ZnO nanorods by wet etching; (c) and (d) top-closed TiO<sub>2</sub> nanotubes with low spin rate (1000 rpm); (e) and (f) top-opened TiO<sub>2</sub> nanotubes with high spin rate (3000 rpm) (insets: (a) the cross-sectional image of ZnO nanorods; (c) top view image of top-closed TiO<sub>2</sub> nanotubes (one fractured tube was captured, clearly showing “tube” structure); (e) the cross-sectional image of top-opened TiO<sub>2</sub> nanotubes; insets of (b), (d), and (f): corresponding images for EDX analysis).

acceptor structure for hybrid metal-oxide/polymer photovoltaic devices.

Before the fabrication of hybrid solar cells, optical properties were observed to understand the nature of the charge transfer between MEH-PPV and TiO<sub>2</sub> nanotubes. Fig. 4(a) shows the typical UV–vis absorption spectra of MEH-PPV, TiO<sub>2</sub> nanotubes, and TiO<sub>2</sub> nanotubes coated with MEH-PPV. The absorption spectrum of MEH-PPV in Fig. 4(a) exhibits the absorption band peak at ~500 nm resulting from the  $\pi \rightarrow \pi^*$  transition of the MEH-PPV. Compared with the absorption spectrum of MEH-PPV, in the case of the TiO<sub>2</sub> nanotubes/MEH-PPV, absorbance was increased without noticeable wavelength shift, caused by the two component contributions. This indicates that the ground-state charge transfer at the interfaces is negligible [52]. Fig. 4(b) shows that the PL emission peak of MEH-PPV appears at ~600–700 nm wavelength, resulting from the

excitation of the MEH-PPV at ~500 nm wavelength. Here, a significant quenching of emission intensity observed in Fig. 4(b) indicates the charge transfer from MEH-PPV to the TiO<sub>2</sub> nanotubes, showing the possibility of an efficient charge separation at the interface between the TiO<sub>2</sub> nanotubes and the MEH-PPV, which ultimately would result in the production of electricity under the illumination of light [53].

Fig. 5 shows the current density–voltage (*J*–*V*) curves of the hybrid solar cells based on the TiO<sub>2</sub> nanotube in combination with MEH-PPV. For a better comparative study, two types of TiO<sub>2</sub> electron acceptors, with and without TiO<sub>2</sub> nanotubes, were prepared. The reference cell with the flat TiO<sub>2</sub> film was prepared by using identical conditions and processes with that of TiO<sub>2</sub> nanotube arrays only except for the electrodeposition process to form ZnO nanorod templates. The inset of Fig. 5 shows the cross-sectional image of the TiO<sub>2</sub> nanotubes, standing perpendicular

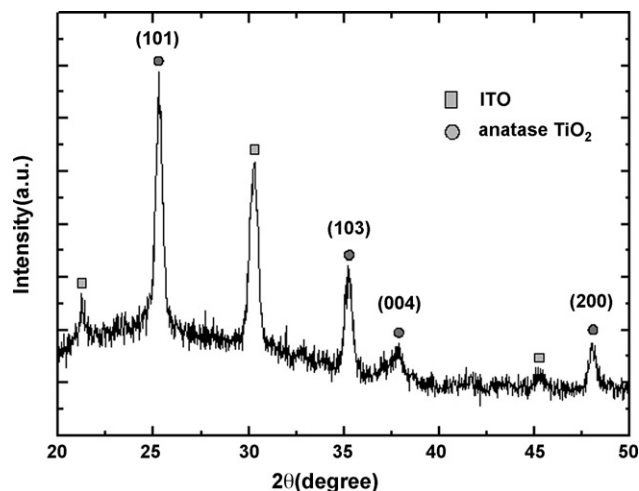


Fig. 3. XRD spectrum of TiO<sub>2</sub> nanotubes on the ITO substrate after heat treatment and removal of ZnO nanorod templates by wet etching.

to the ITO substrate, having diameters of  $\sim 100$  nm and heights  $\sim 300$  nm. The ZnO nanorod template for high efficiency of hybrid solar cells was determined by varying the concentration of the Zn precursor and the electrodeposition time. When the

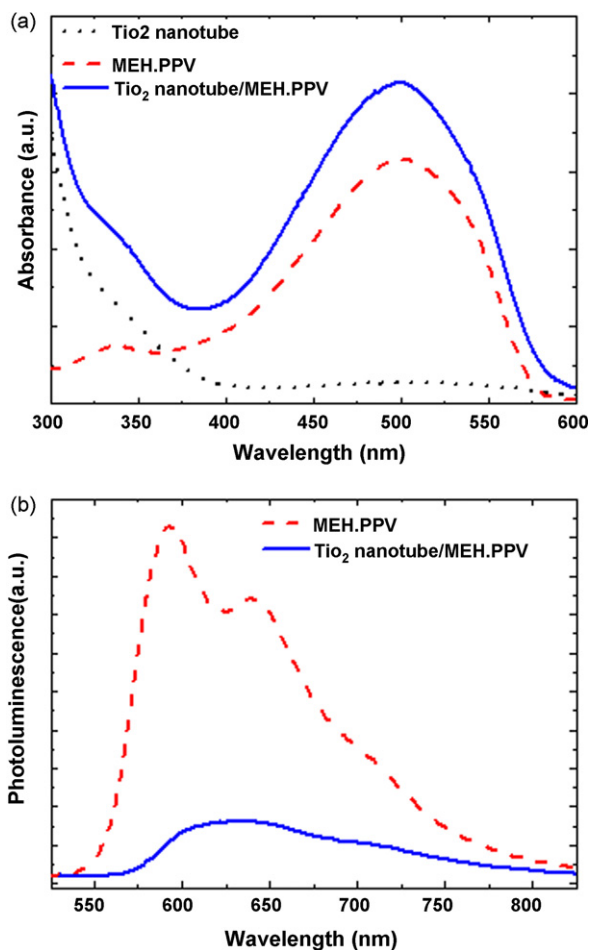


Fig. 4. (a) UV/vis absorption spectra of MEH-PPV, TiO<sub>2</sub> nanotube, and TiO<sub>2</sub> nanotube/MEH-PPV films. (b) PL spectra of MEH-PPV and TiO<sub>2</sub>/MEH-PPV films.

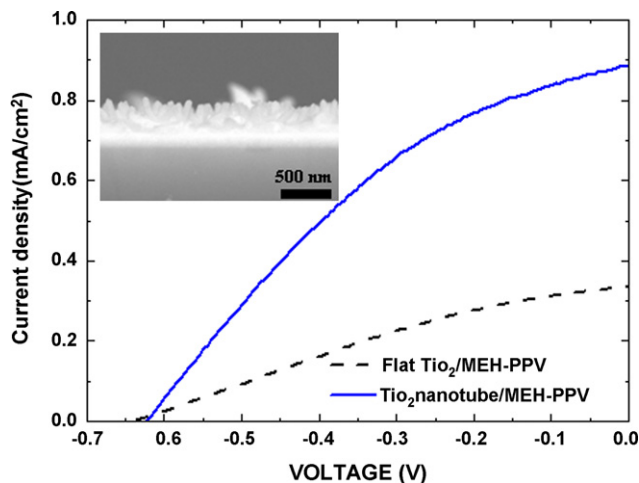


Fig. 5.  $J$ - $V$  curves of hybrid solar cells with the flat TiO<sub>2</sub> film and the TiO<sub>2</sub> nanotube as electron acceptor layers, respectively (inset: the cross-sectional image of the TiO<sub>2</sub> nanotube).

applied electrodeposition time was too long or the concentration of the Zn precursor was too small, the cells showed all poor performance. A maximum efficiency was obtained at the applied time of 15 min and the concentration of the Zn precursor of  $5 \times 10^{-4}$  M ZnCl<sub>2</sub>. The PEDOT:PSS layer was deposited on the MEH-PPV incorporated TiO<sub>2</sub> to reduce surface roughness by filling the voids in the composite films, resulting in the reduction of shunt losses. As demonstrated by the  $J$ - $V$  curves in Fig. 5, an open circuit voltage ( $V_{oc}$ ) of 0.62 V, a short circuit current ( $J_{sc}$ ) of 0.88 mA/cm<sup>2</sup>, a fill-factor (FF) of 37.2%, and a power conversion efficiency ( $\eta_p$ ) of 0.20% were obtained for the TiO<sub>2</sub> nanotubes and the MEH-PPV hybrid solar cell under 1 sun with air mass 1.5 Global illumination without any optimization of the processes such as a metal electrode or an annealing process. On the other hand, the cell with the flat TiO<sub>2</sub> film exhibited  $V_{oc}$  of 0.64 V,  $J_{sc}$  of 0.34 mA/cm<sup>2</sup>, FF of 31.5%, and  $\eta_p$  of 0.068%, respectively. The increased efficiency of the cell using well-aligned TiO<sub>2</sub> nanotubes as an electron acceptor can be attributed to the increased interfacial area for the charge separation and efficient charge transport compared to the flat TiO<sub>2</sub> film. Even though the  $\eta_p$  of the cell with TiO<sub>2</sub> tubes is about three times higher compared with the flat TiO<sub>2</sub> film, the present cell performance is similar to the previous reports of TiO<sub>2</sub> nanoparticle/MEH-PPV hybrid solar cells [54,55]. The insufficient performance of our cell is attributed to the large diameter and relatively low density of the TiO<sub>2</sub> tubes employed in this study, resulting in a lower surface area and the relatively inefficient charge separation, compared with the nanoparticles used in those reports. To achieve higher efficiency in a solar cell, the diameter and height of the tubes should be optimized with consideration for the following three factors: (1) The polymer exciton diffusion length is  $\sim 10$ – $20$  nm, wherein the photogenerated excitons will be more likely to recombine before reaching to the polymer/TiO<sub>2</sub> tube interface for dissociation [54]. (2) A hole mobility would be enhanced with pore diameters in the range of 50–75 nm [56]. (3) As the height of the tube increases, so do the shunt losses of the cell through direct contact between the TiO<sub>2</sub>

tubes and the metal top electrode [57]. However, compared to the limited charge transport in the electron accepting network, which is formed by randomly interspersing TiO<sub>2</sub> nanoparticles, a more efficient charge separation and charge transport would be expected when an optimized geometrical arrangement of the electron accepting TiO<sub>2</sub> tubes is achieved [49–51,58].

#### 4. Conclusions

In summary, this study successfully demonstrated high-density arrays of vertically well-aligned TiO<sub>2</sub> nanotubes on ITO substrates by a simple and controllable fabrication method via the electrodeposition of ZnO nanorod templates and the spin-on based sol–gel reaction of Ti-precursor. This novel method possesses several advantages: it is a simple, fast, and low cost process; there is enhanced flexibility for control of the shape, width, heights, and density of TiO<sub>2</sub> nanotubes; it is feasible to apply them directly on widely used ITO substrates; and they are capable of a large-area fabrication with good uniformity (typically 2 cm × 2 cm under our conditions). The potential for useful applications of the TiO<sub>2</sub> nanotubes was studied by fabricating the hybrid solar cells based on the TiO<sub>2</sub>/MEH-PPV. The power conversion efficiency of the cell with TiO<sub>2</sub> tubes was enhanced compared to that of the cell with flat TiO<sub>2</sub> film due to the extension of the interfacial area available for photo-induced charge separation and charge transport. This method for fabrication of well-aligned TiO<sub>2</sub> nanotube arrays can provide us with new features and applications in opto- and electronic devices.

#### Acknowledgments

This work was financially supported by Heeger Center for Advanced Materials (HCAM), the Ministry of Education of Korea through Brain Korea 21 (BK 21) program, the Korea Science and Engineering Foundation (KOSEF) through the National Research Lab. Program funded by Korean Government (MOST) (M10500000077-06J0000-07710), and MOCIE (Ministry of Commerce, Industry and Energy of the Korean Government) (10022811).

#### References

- [1] S. Iijima, *Nature* 354 (1991) 56.
- [2] J. Goldberger, R. He, Y. Zhang, S. Lee, H. Yan, H.-J. Choi, P. Yang, *Nature* 422 (2003) 599.
- [3] Z. Wang, G. Chumanov, *Adv. Mater.* 15 (2003) 1285.
- [4] Y.-G. Guo, J.-S. Hu, H.-P. Liang, L.-J. Wan, C.-L. Bai, *Adv. Funct. Mater.* 15 (2005) 196.
- [5] G.R. Patzke, F. Krumeich, R. Nesper, *Angew. Chem.* 114 (2002) 2554.
- [6] H. Shin, D.-K. Jeong, J. Lee, M.M. Sung, J. Kim, *Adv. Mater.* 16 (2004) 1197.
- [7] Y. Wang, J.Y. Lee, H.C. Zeng, *Chem. Mater.* 17 (2005) 3899.
- [8] X.-P. Shen, A.-H. Yuan, Y.-M. Hu, Y. Jiang, Z. Xu, Z. Hu, *Nanotechnology* 16 (2005) 2039.
- [9] J.M. Macák, H. Tsuchiya, P. Schmuki, *Angew. Chem. Int. Ed.* 44 (2005) 2100.
- [10] M. Adachi, Y. Murata, M. Harada, S. Yoshikawa, *Chem. Lett.* 29 (2000) 942.
- [11] S. Uchida, R. Chiba, M. Tomiha, N. Masaki, M. Shirai, *Electrochemistry* 70 (2002) 418.
- [12] J.M. Macak, M. Zlamal, J. Krysa, P. Schmuki, *Small* 3 (2007) 300.
- [13] Y. Lan, X. Gao, H. Zhu, Z. Zheng, T. Yan, F. Wu, S.P. Ringer, D. Song, *Adv. Funct. Mater.* 15 (2005) 1310.
- [14] B.D. Yao, Y.F. Chan, X.Y. Zhang, W.F. Zhang, Z.Y. Yang, N. Wang, *Appl. Phys. Lett.* 82 (2003) 281.
- [15] A. Michailowski, D. AlMawlawi, G.S. Cheng, M. Moskovits, *Chem. Phys. Lett.* 349 (2001) 1.
- [16] M.S. Sander, M.J. Côté, W. Gu, B.M. Kile, C.P. Tripp, *Adv. Mater.* 16 (2004) 2052.
- [17] J.H. Lee, I.C. Leu, M.C. Hsu, Y.W. Chung, M.H. Hon, *J. Phys. Chem. B* 109 (2005) 13056.
- [18] J. Qiu, Z. Jin, Z. Liu, X. Liu, G. Liu, W. Wu, X. Zhang, X. Gao, *Thin Solid Films* 515 (2007) 2897.
- [19] J. Qiu, W. Yu, X. Gao, X. Li, *Nanotechnology* 17 (2006) 4695.
- [20] Z.R. Tian, J.A. Voigt, J. Liu, B. McKenzie, H. Xu, *J. Am. Chem. Soc.* 125 (2003) 12384.
- [21] A. Ghicov, J.M. Macak, H. Tsuchiya, J. Kunze, V. Haeublein, L. Frey, P. Schmuki, *Nano Lett.* 6 (2006) 1080.
- [22] S. Bauer, S. Kleber, P. Schmuki, *Electrochem. Commun.* 8 (2006) 1321.
- [23] J.M. Macak, H. Tsuchiya, S. Berger, S. Bauer, S. Fujimoto, P. Schmuki, *Chem. Phys. Lett.* 428 (2006) 421.
- [24] M. Fu, J. Zhou, Q. Xiao, B. Li, R. Zong, W. Chen, J. Zhang, *Adv. Mater.* 18 (2006) 1001.
- [25] C. Lévy-Clément, R. Tena-Zaera, M.A. Ryan, A. Katty, G. Hodes, *Adv. Mater.* 17 (2005) 1512.
- [26] J. Weng, Y. Zhang, G. Han, Y. Zhang, L. Xu, J. Xu, X. Huang, K. Chen, *Thin Solid Films* 478 (2005) 25.
- [27] A. Goux, T. Pauporté, J. Chivot, D. Lincot, *Electrochim. Acta* 50 (2005) 2239.
- [28] S.-S. Kim, C. Chun, J.-C. Hong, D.-Y. Kim, *J. Mater. Chem.* 16 (2006) 370.
- [29] D.K. Yi, S.J. Yoo, D.-Y. Kim, *Nano Lett.* 2 (2002) 1101.
- [30] H. Spanggaard, F.C. Krebs, *Sol. Energy Mater. Sol. Cells* 83 (2004) 125.
- [31] J. Bouclé, P. Ravirajan, J. Nelson, *J. Mater. Chem.* 17 (2007) 3141.
- [32] K.M. Coakly, Y. Liu, C. Goh, M.D. McGehee, *Mater. Res. Bull.* 30 (2005) 37.
- [33] M.S. White, D.C. Olson, S.E. Shaheen, N. Kopidakis, D.S. Ginley, *Appl. Phys. Lett.* 89 (2006) 143517.
- [34] D.C. Olson, S.E. Shaheen, M.S. White, W.J. Mitchell, M.F.A.M. van Hest, R.T. Collins, D.S. Ginley, *Adv. Funct. Mater.* 17 (2007) 264.
- [35] Y. Liu, S.R. Scully, M.D. McGehee, J. Liu, C.K. Luscombe, J.M.J. Fréchet, S.E. Shaheen, D.S. Ginley, *J. Phys. Chem. B* 110 (2006) 3257.
- [36] M. Lira-Cantu, K. Norrman, J.W. Andreasen, N. Casan-Pastor, F.C. Krebs, *J. Electrochem. Soc.* 154 (2007) B508.
- [37] M. Lira-Cantu, K. Norrman, J.W. Andreasen, F.C. Krebs, *Chem. Mater.* 18 (2006) 5684.
- [38] F.C. Krebs, J.E. Carlé, N. Cruys-Bagger, M. Andersen, M.R. Lilliedal, M.A. Hammond, S. Hvidt, *Sol. Energy Mater. Sol. Cells* 86 (2005) 499.
- [39] R. Könenkamp, K. Boedecker, M.C. Lux-Steiner, M. Poschenrieder, F. Zenia, C. Levy-Clement, S. Wagner, *Appl. Phys. Lett.* 77 (2000) 2575.
- [40] M. Kim, B. Kang, S. Yang, C. Drew, L.A. Samuelson, J. Kumar, *Adv. Mater.* 18 (2006) 1622.
- [41] Q. Fan, B. McQuillin, D.D.C. Bradely, S. Whitelegg, A.B. Seddon, *Chem. Phys. Lett.* 347 (2001) 325.
- [42] G. Carcano, M. Ceriani, F. Soglio, *Hybr. Circ.* 32 (1993) 12.
- [43] M. Lira-Cantu, F.C. Krebs, *Sol. Energy Mater. Sol. Cells* 90 (2006) 2076.
- [44] Z. Xie, B.M. Henry, K.R. Kirov, H.E. Smith, A. Barkhouse, C.R.M. Grovenor, H.E. Assender, G.A.D. Briggs, G.R. Webster, P.L. Burn, M. Kano, Y. Tsukahara, *Thin Solid Films* 511/512 (2006) 523.
- [45] M.Y. Song, J.K. Kim, K.-J. Kim, D.Y. Kim, *Synth. Met.* 137 (2003) 1387.
- [46] M.Y. Song, K.-J. Kim, D.Y. Kim, *Sol. Energy Mater. Sol. Cells* 85 (2005) 31.
- [47] P.A. van Hal, M.M. Wien, J.M. Kroon, W.J.H. Verhees, L.H. Slooff, W.J.H. van Gennip, P. Jonkheijm, R.A.J. Janssen, *Adv. Mater.* 15 (2003) 118.
- [48] P. Ravirajan, S.A. Haque, J.R. Durrant, D. Poplavskyy, D.D.C. Bradely, J. Nelson, *J. Appl. Phys.* 95 (2004) 1473.
- [49] K.M. Coakley, M.D. McGehee, *Appl. Phys. Lett.* 83 (2003) 3380.

- [50] D.C. Olson, J. Pirus, R.T. Collins, S.E. Shaheen, D.S. Ginley, *Thin Solid Films* 496 (2006) 26.
- [51] Q. Wei, K. Hirota, K. Tajima, K. Hashimoto, *Chem. Mater.* 18 (2006) 5080.
- [52] N.C. Greenham, X. Peng, A.P. Alivisatos, *Phys. Rev. B* 54 (1996) 17628.
- [53] A. Petrella, M. Tamborra, M.L. Curri, P. Cosma, M. Striccoli, P.D. Cozzoli, A. Agostiano, *J. Phys. Chem. B* 109 (2005) 1554.
- [54] P. Ravirajan, S.A. Haque, J.R. Durrant, D.D.C. Bradley, J. Nelson, *Adv. Funct. Mater.* 15 (2005) 609.
- [55] A.J. Breeze, Z. Schlesinger, S.A. Carter, *Phys. Rev. B* 64 (2001) 125205.
- [56] K.M. Coakley, B.S. Srinivasan, J.M. Ziebarth, C. Goh, Y. Liu, M.D. McGehee, *Adv. Funct. Mater.* 15 (2005) 1927.
- [57] P. Ravirajan, A.M. Peiro, M.K. Nazeeruddin, M. Graetzel, D.D.C. Bradley, J.R. Durrant, J. Nelson, *J. Phys. Chem. B* 110 (2006) 7635.
- [58] T.-W. Zeng, Y.-Y. Lin, H.-H. Lo, C.-W. Chen, C.-H. Chen, S.-C. Liou, H.-Y. Huang, W.-F. Su, *Nanotechnology* 17 (2006) 5387.